Journal of Hydrology 388 (2010) 131–143

Contents lists available at ScienceDirect

Journal of Hydrology

journal homepage: www.elsevier.com/locate/jhydrol

An extreme value analysis of UK drought and projections of change in the future

Eleanor J. Burke *, Richard H.J. Perry, Simon J. Brown

Met Office Hadley Centre, FitzRoy Road, Exeter EX1 3PB, UK

ARTICLE INFO

Article history:
Received 30 September 2009
Received in revised form 16 April 2010
Accepted 23 April 2010

This manuscript was handled by
A. Bardossy, Editor-in-Chief, with the
assistance of Efrat Morin, Associate Editor

Keywords:
Drought
Climate change
Extreme value analysis

SUMMARY

Extreme value analysis of drought indices was used to assess the likelihood of drought over the UK during the 20th century and potential future changes due to increased atmospheric greenhouse gasses. Precipitation indices were derived using 3, 6, 12 and 18 month accumulations, normalised by the 1961–1990 mean and standardized by the corresponding standard deviation. A soil moisture index, similarly standardized, was calculated from monthly soil moisture data. Output from an 11-member perturbed physics ensemble of the Hadley Centre regional climate model (HadRM3), forced at the boundaries by equivalent versions of the Hadley Centre global climate model (HadCM3), was evaluated against available observational-based reference data. Soil moisture reference data were derived from a distributed land surface scheme driven by meteorological reanalysis. Whilst the model ensemble underestimates the variability of the precipitation climatology in the reference data, it accurately replicates the extreme characteristics of dry months for the majority of the ensemble members. Differences in land surface characteristics and the representation of sub-grid scale heterogeneity means that there are significant differences in the representation of soil moisture between model and reference data. However, when HadRM3 is forced at the boundaries by ERA-40 reanalysis data the extreme characteristics of low soil moisture are replicated by the model ensemble indicating that using the regional climate model ensemble to downscale from the coarse resolution of HadCM3 is appropriate. Projections of drought for the 21st century were estimated by applying non-stationary extreme value theory to these monthly drought indices. All drought indices show an overall increase in drought in the future. However, the spread of values is considerable ranging from little change or a slight decrease to a significant increase depending on ensemble member and, to a smaller extent, location. The impact of these projections are put in the context of the notorious UK drought of the summer of 1976. This work provides preliminary steps towards a probabilistic assessment of changes in future drought.

1. Introduction

Drought events are rare events which can have a significant socio-economic impact on local communities and nations. Drought develops during or following periods of low accumulated precipitation relative to normal conditions and is exacerbated by high temperatures. As a drought develops, the lack of rainfall leads to persistently dry conditions, low soil moisture, low river flows, reduced storage in reservoirs and less groundwater recharge (Tallaksen and van Lanen, 2004).

In the UK, the 1976 summer drought was a notoriously high impact event with the national press calling it the 'Great Drought'. The 16-months between May 1975 and August 1976 had the lowest 16-month rainfall since records began in 1766. In addition, the majority of British rivers had their lowest flows on record (Marsh et al., 2007). Impacts included forest fires in Southern England which destroyed up to 50,000 trees, crop failure resulting in £500 million worth of losses and widespread water rationing with public standpipes in some areas (Currie, 2008; Herbert, 2006; Wainwright, 2006). A Drought Act was passed by the UK government and a minister was made responsible for handling the water shortage. It is important to know how the likelihood of droughts, such as the 1976 event, will change in the future to allow effective water resource strategies and drought action plans to be developed.

Global climate models (GCMs) can be used to assess the possible change in the likelihood of drought in the future by modelling the effect of particular future emission scenarios of greenhouse gasses on the climate. Generally, GCMs are of low resolution so in order to provide spatially detailed local information, over the UK for example, they need to be combined with a downscaling technique. Two main downscaling approaches exist (Fowler et al., 2007). The first is a set of statistical techniques where empirical relationships between the GCM-resolution climate and the local climate are derived. However, this assumes that the statistical relationships from the 20th century are the same as those in the

* Corresponding author. Tel.: +44 1392 884231; fax: +44 (0) 1392 885681.
E-mail address: eleanor.burke@metoffice.gov.uk (E.J. Burke).

0022-1694/$ - see front matter Crown Copyright © 2010 Published by Elsevier B.V. All rights reserved.
doi:10.1016/j.jhydrol.2010.04.035

future and it is hard to capture changes in variability and extremes (Fowler et al., 2007). The second is a dynamical downscaling approach where a higher resolution regional climate model (RCM) is nested within the GCM. It is generally assumed that regional processes do not affect the large scale atmospheric flow so only one way nesting is applied. These models are physically based and as such dynamically reproduce extreme events and any future changes in their nature.

Deficiencies in an individual climate model (regional or global) may adversely affect the simulated climatology and any projected future changes. Therefore, if future projections are to provide credible guidance to adaptation strategies their uncertainties must be adequately characterised. Uncertainties arising from the actual modelling of the physical climate and natural variability can be characterised through the use of model ensembles. For example, multi-model ensembles have been extensively used (e.g. Christensen et al., 2007) as have approaches based on perturbing uncertain parameters in a single model (Murphy et al., 2004). Clark et al. (2006) and Barnett et al. (2006) used a perturbed physics GCM ensemble to project an increase in extremely hot events under increased atmospheric CO_2. They found large uncertainties in the size of the increase dependent on ensemble member. Another factor affecting the projection of any future changes is the nature of future emissions. In order to incorporate these types of uncertainties, methods for probabilistic assessments of climate change are currently being developed. Probabilistic projections have employed probability density functions (pdfs) of global mean warming (Meehl et al., 2007; Murphy et al., 2004; Stainforth et al., 2005). These were produced by weighting the performance of members of ensembles against their ability to represent the historic climate. Pdfs have also been produced for regional scale changes (e.g. Stott, 2003; Tebaldi et al., 2004) with some specifically applicable to hydrological assessments (Ekstrom et al., 2007; Hingray et al., 2007). The UKCP09 program (http://www.ukcip.org.uk), has provided probabilistic projections over the UK for a range of climate variables (Murphy et al., 2009) and the work discussed in this paper is a step towards using this methodology for probabilistic projections of drought over the UK. It develops methods for assessing projected changes of drought using a perturbed physics regional climate model ensemble and tools that can be adopted to produce pdfs of drought recurrence in the future.

Previous research into projected changes in drought over the UK have used multi-model GCM ensembles downscaled either dynamically (Blenkinsop and Fowler, 2007) or statistically (Vidal and Wade, 2009). Despite some limitations on the ability of their RCMs to simulate the observed frequency of drought events, Blenkinsop and Fowler (2007) project an increase in short-term summer drought in England and Wales. They also suggest that the longest drought events will become shorter and less severe. Their results are highly uncertain and strongly dependent upon the driving GCM. Similarly, Vidal and Wade (2009) project an increase in the frequency of short term drought events, a decrease in long term drought, and advise the use of model ensembles for water resource planning. These studies focus on precipitation based drought metrics for a limited number of ensemble members. Here we additionally discuss a soil moisture-based drought index.

The most extreme events have the greatest impact but by definition these are the most rare and are difficult to characterise statistically. The application of extreme value theory and the fitting of extreme distributions to address this difficulty is becoming increasingly common in climate studies (Kharin and Zwiers, 2000; Wettstein and Mearns, 2002; Zhang et al., 2004; Kharin et al., 2007). The few studies which have investigated extreme value distributions in a changing climate have focused on short duration events such as daily temperature or daily precipitation extremes (for example, Nogaj et al., 2006; Brown et al., 2008; Tomassini and Jacob, 2009; Sugahara et al., 2009).

This paper applies extreme value theory to drought indices that represent dry conditions over periods of 1–18 months to quantify the occurrence of extreme drought. The ability of HadRM3 to reproduce historic drought over the UK is assessed and projections of changes in the future are made. These changes are put in the context of the severe drought that occurred for much of the UK in the summer of 1976. In the future the method developed here will form the basis of a methodology for probabilistic projections of drought.

2. Definition of drought

Drought was defined using both precipitation and soil moisture based indices. Monthly accumulations of precipitation from the previous 3, 6, 12 and 18 months were used to define monthly drought indices. Accumulated precipitation was used because drought has a greater impact over time scales longer than 1 month. Additionally, the likelihood of zero precipitation in any month needs to be negligible in order to use extreme value analysis. The minimum value over the period of record of the 3-month accumulations was 5 mm. In some regions over the UK short term (3–6 month) drought has considerable impact on water resources, whereas in others long term (12 to longer than 18 months) has a greater impact. These monthly accumulations of precipitation were converted to monthly drought indices (D_t) by calculating the standardized anomalies from climatology:

$$D_t = \frac{(P_t - P_t^{c\lim})}{\sigma_{P_t^{c\lim}}} \text{ with } P_t = \sum_{i=1}^{t} p_i \quad (1)$$

where p_i is the monthly precipitation for month i; t is the time over which there is an accumulation for each month i; P_t is the accumulated precipitation over time t; $P_t^{c\lim}$ is the climatology of the mean precipitation accumulation over time t for the period 1961–1990. Similarly $\sigma_{P_t^{c\lim}}$ is the standard deviation of the precipitation accumulation climatology over time t, again for the period 1961–1990. This definition of drought preserves the statistical properties of dry months present in the original data. The drought indices for 3, 6, 12 and 18 months precipitation accumulations are D_3, D_6, D_{12}, and D_{18} respectively. The drought indices have little statistical dependence on the time of year allowing the indices from all months to be pooled for analysis. This results in an improved data sample for the application of the extreme value methodology discussed in Section 4.

A monthly soil moisture drought index D_{sm} was defined by the standardized anomalies of the monthly soil moisture (cf. Eq. (1) for $t = 1$). As before, climatology was taken to be the monthly mean and standard deviation of the 1961–1990 soil moisture. Drought indices defined from accumulated soil moisture (i.e. $t > 1$) were not included within this analysis because, unlike precipitation, soil moisture already retains some memory of previous months. This is reflected by serial correlations or memory of between 0.3 and 0.8 for 1-month lag time; with the amount of memory depending on the region under consideration. As well as removing much of the seasonality from the drought indices these standardized anomalies enable comparison between different measures of soil moisture. For example, Wang et al. (2009) and Koster et al. (2009) show that the soil moisture output from an ensemble of different land surface schemes driven by observed meteorological forcing have very distinct magnitudes and seasonality. However, when they are standardized they produce approximately comparable information on temporal variability.

3. Data

3.1. Hadley centre climate models

The model simulations used here were made with version 3 of the Hadley Centre Climate model (HadCM3 – Gordon et al., 2000) which has an atmospheric resolution of 2.5° latitude by 3.75° longitude corresponding to ~300 km at the equator with 19 levels in the vertical. The atmosphere is coupled to a fully dynamical ocean with a resolution of 1.25° by 1.25°. HadCM3 incorporates the Met Office Surface Exchanges Scheme (MOSES) which calculates water and energy fluxes at the land surface (Cox et al., 1999). A single energy and water balance is calculated for each grid cell, based on one set of effective parameters which represent the combination of different land cover types within that grid cell. MOSES has four layers with depths chosen to capture the important temperature cycles. Soil hydrology is based on these four layers and an approximation to the Richard's equation (Cox et al., 1999). Effective soil physical parameters are calculated from the different soil types in the grid cell. Plant physiological processes including photosynthesis, respiration and transpiration are also represented within the model.

HadCM3 has only four land grid points over the UK so in order to provide more detailed spatial information for the UK it is necessary to implement a downscaling technique. In this case the Hadley centre regional climate model (HadRM3) was used. HadRM3 uses a rotated pole grid with a resolution of 25 km and 19 levels in the vertical (Jones et al., 2004). It is parallel to HadAM3 (Pope et al., 2000) except for the resolution dependent parameters which have been tuned to 25 km. HadRM3 can be forced at the boundaries by either output from a global climate model or by an atmospheric reanalysis such as ERA-40 (Uppala et al., 2005). The regional climate model was run over Europe, although only the UK has been analysed in this paper. Output from HadRM3 includes monthly precipitation and monthly soil moisture which are used to calculate the drought indices defined above. This paper presents results from HadRM3 forced at the boundaries by ERA-40 atmospheric reanalysis and from an eleven member perturbed physics ensemble based on HadRM3 with lateral boundary conditions from HadCM3 (Murphy et al., 2009).

3.2. HadRM3 forced by ERA-40

Synoptic scale variability within HadRM3 is largely determined by the boundary forcing. Hence any errors in the large scale atmospheric flow of the forcing data will also be present in the regional climate model run. Therefore, to fully assess the downscaling ability of HadRM3, the reference data (see Section 3.4) are compared with output from an RCM forced at the boundaries by the ERA-40 global atmospheric reanalysis data denoted RM40. As such reanalyses are based on assimilating all possible observations they represent the best available estimate of historical global atmospheric conditions. RM40 output is available for the same time period as the ERA-40 reanalysis data (1958–2002). It should be noted that any differences between RM40 and the reference data may also be a result of errors in the ERA-40 reanalysis.

3.3. Perturbed physics ensemble

Here an 11-member perturbed physics ensemble is used in which each ensemble member consists of a perturbed physics version of HadRM3 forced at the boundaries by the equivalent perturbed physics version of HadCM3. One member, the standard published version (Gordon et al., 2000), has no parameter perturbations and is the same configuration as for RM40 above. The other members have multiple parameter perturbations discussed in detail in Collins et al. (2009) and summarised in the paragraph below. The perturbed HadCM3 models yield simulations of global climate of comparable quality to the standard published version of HadCM3 (Collins et al., 2009). Each ensemble member is run from 1950 to 2100. For the historical period the most important external climate forcings are included in the driving GCM and RCM (Collins et al., 2009). For the future period they are run under the A1B (medium) emissions scenario with constant solar forcing and volcanic aerosol (Murphy et al., 2009).

A selection of 31 uncertain parameters were perturbed in combination away from their standard value but within uncertainty ranges specified by experts. These parameters directly influence the following processes: large scale cloud, convection, radiation, boundary layer, dynamics, land surface processes and sea ice (Collins et al., 2009). The combination of multiple parameter perturbations were chosen to cover a range of climate sensitivity whilst retaining skill in reproducing the historic climate (Webb et al., 2006; Murphy et al., 2004). The main parameter which directly affects soil moisture is one which determines the plant rooting depth: a smaller rooting depth parameter means less soil water available for the plant to extract from the soil and vice versa. This is found to significantly impact the serial correlation of the soil moisture. The standard value, which is also used for RM40, is the deepest rooting depth with the longest serial correlation.

3.4. Reference data

The ability of the 11-member HadRM3 ensemble to recreate precipitation drought during the 20th century (historic) was tested by comparison with reference data derived from observations. Monthly precipitation data gridded at 5 km resolution are available for the period between 1914 and 2005 on the GB national grid. These data were created from station precipitation measurements which were interpolated to the 5 km grid by regressing the normalised precipitation with geographic factors such as topography and then interpolating the model residuals (Perry and Hollis, 2005). These were re-projected and then re-gridded using bilinear interpolation to a rotated pole grid of 25 km resolution so they were comparable with the regional climate model output.

Gridded in situ soil moisture observations are unavailable, therefore the ability of the climate model to reproduce observed in situ soil moisture cannot be validated directly. However, a model-derived substitute can be used to give an indication of the observed soil moisture and the performance of the regional climate model. This was obtained from a different version of MOSES to that incorporated within the climate models (MOSES-PDM) which explicitly includes sub-grid scale heterogeneity of both land cover and soil hydrology by incorporating a Probability Distributed Moisture scheme (PDM). MOSES-PDM was driven by historical meteorological data from the Met Office's Nimrod nowcasting system (Golding, 1998) for the period 1960–2005 (Smith et al., 2006) and is denoted here by MPDM. Since MPDM uses analyses of observed meteorology, the spatial and temporal distributions of dry periods are expected to be well represented. MPDM has been validated at two locations in south-east England; a grassland site on a medium soil and a woodland site on a coarse soil (Blyth, 2002). The model did remarkably well for both cases calculating a reasonable mean soil moisture and seasonal variation. The output from MPDM is soil moisture deficit where a large deficit means dry conditions. This is different to the regional climate model output which calculates available soil moisture – a small available soil moisture means dry conditions. Therefore the climatologies are not directly comparable. However, the standardization process used to derive the drought indices enables a useful evaluation of any differences

Table 1
Summary of the datasets used in this paper.

Metric	Data set	Time period	Source
Precipitation	Reference	1914–2005	Gridded observations (Perry and Hollis, 2005)
Precipitation	RM40	1958–2002	Standard version of HadRM3 forced by ERA-40 reanalysis
Precipitation	HadRM3	1950–2100	11 perturbed physics versions of HadRM3 each forced by equivalently perturbed HadCM3
Soil moisture	Reference	1960–2005	MOSES-PDM (Smith et al., 2006)
Soil moisture	RM40	1958–2002	Standard version of HadRM3 forced by ERA-40 reanalysis
Soil moisture	HadRM3	1950–2100	11 perturbed physics versions of HadRM3 each forced by equivalently perturbed HadCM3

between the reference data and the regional climate model to be made.

For clarity, Table 1 summarises the datasets used in this paper.

4. Methodology

4.1. Climate model evaluation

The climate model was evaluated by comparing both the RM40 simulation and the HadRM3 ensemble with the reference data. First the ability of the model to replicate the mean and standard deviation of the reference precipitation climatology was studied. The climatology of MPDM soil moisture cannot be directly compared with HadRM3 or RM40 soil moisture because they are based on different definitions. Second, the Pearson Correlation Coefficient between RM40 drought indices and the reference drought indices was calculated on a grid cell basis to see how temporal variability compares. This is only possible for RM40 and not the HadRM3 simulations because RM40 is driven at the boundaries by meteorological reanalysis which represent 20th century natural variability whereas the HadRM3 simulations are driven by HadCM3 which generates its own natural variability. This enables an assessment of the degree to which RCM drought variability is driven by the large scale atmospheric flow. The ability of the climate model to reproduce the distribution of the reference drought indices was also tested on a grid cell basis using the Kolmogorov–Smirnoff test. Finally extreme value theory was applied to evaluate the ability of the RCM to replicate the characteristics of dry months. This approach is discussed in detail below.

4.2. Extreme value statistics

This paper applies extreme value analysis to the monthly drought indices in order to explore the statistical behaviour of dry months for the reference data; the 20th century; and the 21st century. The three applications discussed are:

1. Determining the characteristics of dry months in the historic record.
2. Assessing whether the characteristics of dry months in HadRM3 are the same as in the historic record.
3. Evaluating the potential changes of the likelihood of dry months in the future as a result of climate changing from increased greenhouse gasses.

A brief discussion of extreme value theory and its application to a monthly drought index follows. It should be noted that, in this discussion, the drought index is inverted and positive values represent the deficit values of dry months (in standardized units).

A peaks-over-threshold model was utilised to describe all deficits of dry months greater than a threshold (u – Coles, 2001). The threshold was selected to retain only a small fraction of the data whilst remaining within the tail of the distribution, but retaining sufficient data to enable a good fit of the extreme value distribution. Here it was set to the 94th percentile of the entire distribution of monthly drought indices. These deficits were assumed to occur according to a Poisson process, and the degree to which the deficits exceed the threshold was assumed to follow a Generalised Pareto distribution (Katz et al., 2002). The extreme value model (EVM) describing the expected number of threshold exceedances per year above any level y, conditional on y being greater than the threshold, u, can be written as:

$$E(n > y | y > u) = \left[1 + \xi\left(\frac{y-\mu}{\sigma}\right)\right]^{-1/\xi} \tag{2}$$

where μ, σ, and ξ are termed the location, scale and shape parameters respectively (Coles, 2001). The location parameter is analogous to the mean of a normal distribution, so any increases in μ uniformly shift the distribution to higher values, whereas the scale and shape parameters determine the rate which the magnitude of extremes alters with rarity. The parameters were estimated by maximum likelihood (Coles, 2001) as this facilitates the inclusion of covariates for the non-stationary parameters and the imposition of constraints to ensure all values are feasible under the estimated distribution. The return level (z_m) is the deficit exceeded on average once every m years, where m is commonly referred to as the return period (Coles, 2001). z_m is given by:

$$\begin{aligned} z_m &= \mu - (\sigma/\sigma\xi)\left\{1 - \left[-\ln\left(1 - \frac{1}{m}\right)\right]\right\}^{-\xi} \quad \xi \neq 0 \\ z_m &= \mu - \sigma \ln\left[-\ln\left(1 - \frac{1}{m}\right)\right] \quad \xi = 0 \end{aligned} \tag{3}$$

Both the return level or deficit for a given return period (in years) and the return period for a given deficit or return level are the descriptors of drought used in this paper. Analysis of the drought indices with the long accumulation times gives an indication of long term drought and those with the short accumulation times gives an indication of short term drought.

All available months of the year were pooled for analysis in order to increase the sample size and improve the fitting of the distribution. Serial correlation in the monthly drought indices was reduced through de-clustering. If two or more consecutive months exceed the threshold they are assumed to belong to the same cluster and only the driest month is included within the sample selected for extreme value distribution fitting. Dry months are also assumed to belong to the same cluster if they are separated by fewer than 2 months of data below the threshold.

The relationship between return level and return period were calculated by fitting an EVM for each grid cell in the reference data. It was assumed that this did not change (i.e. the relationship is stationary) over the period of record and thus the location, scale and shape parameters were independent of time.

The EVM described above can be extended to account for non-stationarity which is useful for comparing the HadRM3 ensemble against the reference data and quantifying changes in dry months in the future. Non-stationarity is modelled by allowing the location, scale and shape parameters to depend either separately or jointly on a covariate, x. The nature of this covariate depends on

the application as discussed below. Here, the parameters are allowed to depend linearly on the covariate in the following way:

$$\mu_t = \alpha_0 + \alpha_1 x \quad (4)$$

$$\sigma_t = \exp(\beta_0 + \beta_1 x) \quad (5)$$

$$\xi_t = \gamma_0 + \gamma_1 x \quad (6)$$

For non-stationary EVM it is necessary to ensures exceedances above the threshold are obtained throughout the data record at a relatively constant rate requiring the threshold to have a similar dependence on the covariate e.g. $u(x)$.

The significance of non-stationarity in the parameters (Eqs. (4)–(6)) was assessed by comparing the quality of the fits made with different EVMs: a stationary EVM ($x = 0$), and three EVMs representing non-stationarity ($x > 0$): first in the location only; then in the location and scale; and finally in all of the location, scale and shape parameters. EVM selection was achieved by means of a likelihood ratio test conducted at the 10% level i.e. an EVM is considered to be statistically superior than a simpler EVM if the deviance between the fitted EVMs (twice the difference in maximised log-likelihoods) exceeds the upper 10% quantile of the chi-squared distribution with the appropriate degrees of freedom (Coles, 2001). The two different applications using non-stationary EVMs are discussed in detail below.

4.2.1. Validating the HadRM3 ensemble over the historic period

Comparisons between each HadRM3 ensemble member and the reference data/RM40 were made independently on a grid point by grid point basis. This was done for the period between 1960 and 2002 for RM40 and 1951 and 2005 for the precipitation reference data and 1960 and 2005 for the soil moisture reference data. Thresholds for exceedances were identified for the model and the reference data separately defined as the 94th percentile of each distribution. The exceedances were then de-clustered and the two data sets pooled. EVMs were fitted based on the assumption that the data came from either one population (where $x = 0$ for both data sets) or two populations ($x = 0$ for reference data and 1 for model). The ensemble member and reference data/RM40 were taken to be statistically identical if the EVM with $x = 0$ for both data sets provided the best fit at that grid point.

4.2.2. Future changes in dry months

The climate model output for the period between 1950 and 2100 was used to determine whether there are any significant changes in dry months in the future; i.e. whether a non-stationary EVM is a better fit than a stationary EVM. Here the covariate (x) of c (4)–(6) is taken to be the global mean temperature. For each ensemble member, this is obtained from the GCM with the same parameter perturbations that was used to provide boundary forcing for that RCM member. In each case the global mean temperature was smoothed using a spline function to remove year to year variability and normalised by the 1950–2100 mean temperature. This measure of global mean temperature was preferred over a simple time dependence because global mean temperature changes are non-linear over the relevant time period and dependent on the ensemble member under consideration (Collins et al., 2009). The non-stationary threshold was obtained by fitting a spline function through all data which are drier than the mean. This fitted curve is then shifted uniformly until it exceeds a predetermined proportion of the data (94% in this case). Exceedances were then de-clustered and EVMs fitted.

Robust identification of non-stationarity in the scale and shape parameters is difficult with all but the longest records. Therefore, in order to improve the sample size and better constrain the EVM form, it was assumed that for each grid cell, all ensemble members have the same form of non-stationarity in the future. In other words, whether or not the parameters defined in Eqs. (4)–(6) depend on the covariate, x is the same for all members in a given grid cell. In order to determine the form of the EVM all the data was pooled and the stationary and all of the non-stationary EVMs were fitted for each grid cell. Given that each ensemble member may have a different drought climatology, first order intra-ensemble differences were removed by subtracting the estimated 94th percentile of the 'present-day' (1950–2005) distribution for that member. It is assumed that the dominant non-stationary characteristics of the data will be unaffected by higher order differences in the different RCM members. The preferred EVMs were restricted to either location or location and scale depending on global temperature since the other EVMs were preferred for less than 10% of the UK with little spatial coherence. The most appropriate of these was then determined by the likelihood ratio test described above. This preferred EVM was then fitted to each of the individual ensemble members separately to provide EVM parameters for each ensemble member at each grid point. Any change in the return period for a given return level (deficit of dry months) was then calculated separately for each member, resulting in a distribution of possible changes.

5. Results

5.1. Comparing modelled and reference climatologies

The characteristics of the precipitation climatologies over the UK are summarised in Fig. 1 (top row) for accumulation times of 12 months (P_{12}). Fig. 1a and c shows the mean and standard deviation (mm/month) of reference P_{12} for the period 1961–1990. The means and standard deviations are lowest in eastern England; higher in the west; and highest in western Scotland reflecting regional topography and prevailing weather. The reference UK average for P_{12} is 88.7 mm/month with a standard deviation of 12.6 mm/month or 14% of the 1961–1990 mean. The reference standard deviation ranges from 30.9 mm/month (35%) for P_3 to 11.6 mm/month (13%) for P_{18}. Fig. 1b and d show comparable plots to Fig. 1a and c, but for RM40. In both cases the spatial patterns are very similar, as might be expected given the dependence of precipitation on topography. In general RM40 has less accumulated precipitation than the reference data in the north and west and slightly more in the south and east. Overall RM40 has a slightly lower area weighted mean (82.1 mm/month) than the reference data (88.7 mm/month) and a slightly lower standard deviation over the majority of the UK, with an overall average of 11.3 mm/month.

The lower half of Fig. 1 demonstrates the ability of the HadRM3 model ensemble to recreate the reference data. Each of the ensemble members is compared to the reference data and for each grid cell the maximum and minimum differences between the ensemble and reference data are shown. [Note: these differences can be from different ensemble members]. In general the ensemble members have between 30% less to 30% more accumulated precipitation than the reference data (Fig. 1e and f). Some of this spread might be expected given the perturbed parameter approach. In small regions of the north-west all of the ensemble members are drier than the reference data (red[1] for both figures) whereas in small regions of the south east all of the ensemble members are wetter (blue for both figures). This mirrors the spatial biases seen when comparing the reference data with RM40 suggesting that there is some downscaling bias in the regional model since RM40 and the ensemble have different boundary conditions. The mean of the reference data

[1] For interpretation of color in Fig. 1, the reader is referred to the web version of this article.

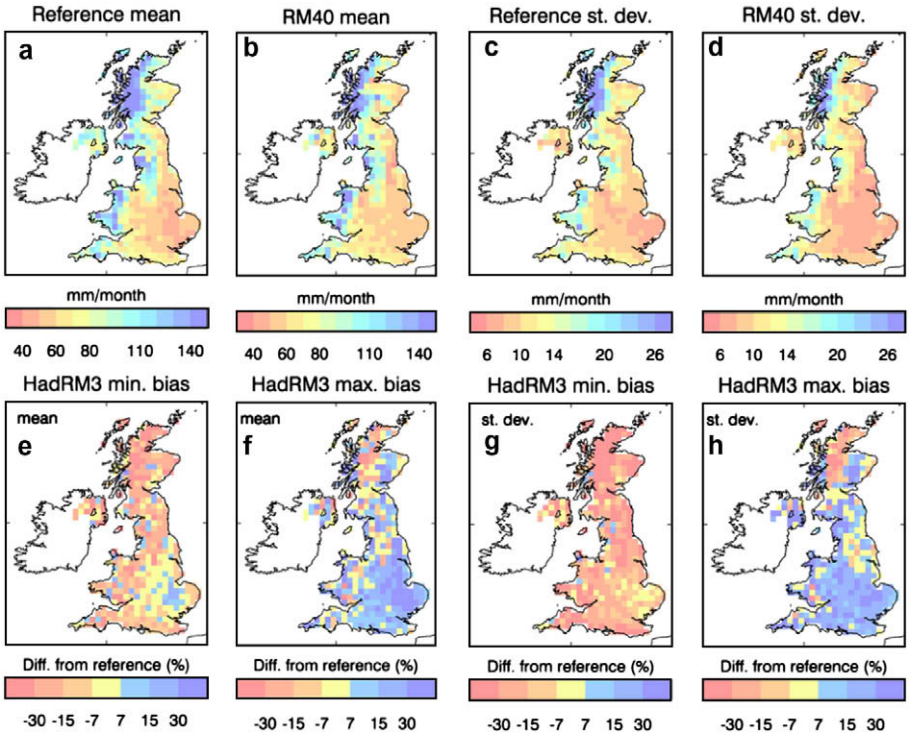

Fig. 1. The mean monthly precipitation from (a) reference data; (b) RM40. The standard deviation of monthly precipitation from (c) reference data; and (d) RM40. Also shown are the difference between the model ensemble and the reference data for the period 1961–1990. (e) and (f) show the ensemble spread for the mean expressed as a percentage of the reference mean; and (g) and (h) show the ensemble spread for the standard deviation expressed as a percentage of the reference standard deviation.

fall within the range of the model ensemble for over 50% of the UK including spatially coherent regions in south-central England and eastern England and Scotland. The reference standard deviation of P_{12} lies within the ensemble spread for 73% of the area including the majority of England and Wales. The main region where the reference data fall outside this range is over north-west Scotland where the model ensemble has a smaller standard deviation than the reference data. This could be a result of unresolved topography in the model. A comparison between RM40 and the HadRM3 model ensemble (not shown) shows excellent agreement with the RM40 mean and standard deviation falling within the spread of the ensemble members for 98% and 88% of the area respectively. Although model soil moisture cannot be compared with the reference data, the mean and standard deviation of the RM40 monthly soil moisture also falls within the spread of the HadRM3 ensemble for nearly all grid cells. This level of agreement between RM40 and the ensemble further suggests the spatial bias with respect to the reference data is most likely because of the downscaling of the regional model and not the boundary conditions. A possible explanation of this bias could be that too little moisture is rained out over the western regions high ground during westerly atmospheric flow resulting in the atmosphere being too moist over the eastern regions and producing excessive rain in the east.

5.2. Comparing modelled and reference drought indices

Fig. 2 shows the point-by-point Pearson Correlation Coefficient between the reference data and the RM40 time series for the drought indices calculated using Eq. (1). Correlations for D_3 and D_{12} are represented in Fig. 2a and b. Correlations for D_6 are very similar to those for D_3 and correlations for D_{18} are very similar to those for D_{12} so these two are not shown. The precipitation drought indices have correlations greater than 0.4 for nearly all of the grid cells, with values of up to 0.8 in some regions. Correlations improve slightly with increasing accumulation times – area mean values are 0.57 for D_3 and 0.61 for D_{18}. Correlations are generally greater in north-west Scotland and south-east England – the areas of highest and lowest precipitation. Fig. 2c shows the correlations for D_{sm}. These correlations are lower than for the precipitation drought indices with typical values between 0.4 and 0.5. These are also noticeably lower in the east than the west. Correlations for D_{sm} might be expected to be lower than for the precipitation drought indices because the differences in the land surface schemes will impact the time series. For example, there are differences in the memory of D_{sm} between the reference data and RM40. This is discussed later in more detail.

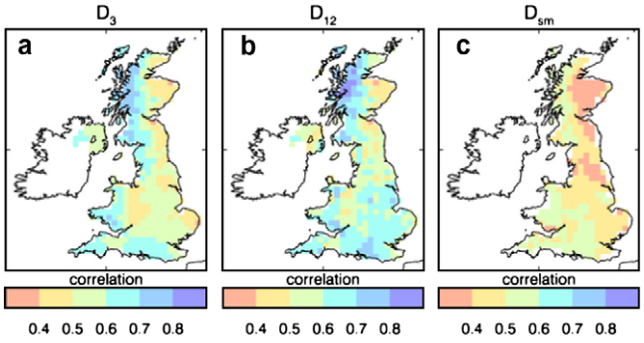

Fig. 2. The point-by-point temporal correlation for each drought index between the reference data and RM40 for (a) 3 month precipitation (D_3); (b) 12 month precipitation (D_{12}); and (c) soil moisture (D_{sm}).

Fig. 3 summarises the results of the Kolmogorov–Smirnoff (K–S) test which compares the distributions of the drought indices. Fig. 3a shows that, for the majority of the UK, at least 75% of the ensemble members have distributions of the D_3 drought index which are indistinguishable from the reference data. In some re-

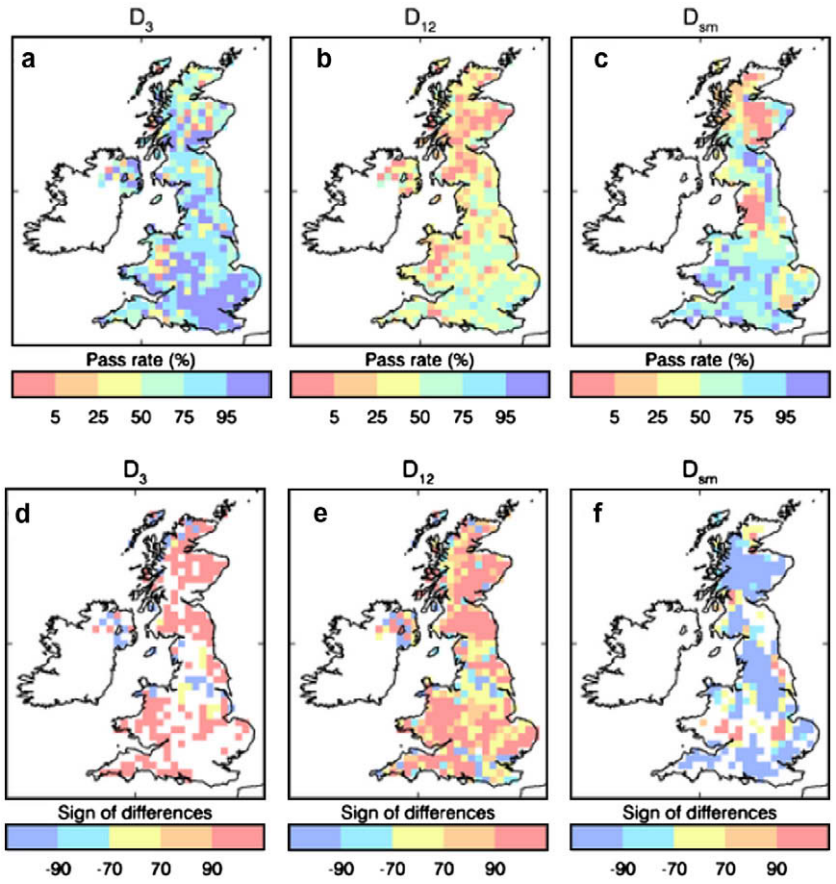

Fig. 3. The comparison of the distributions of model ensemble and the reference data. The percentage of the models which pass the Kolmogorov–Smirnoff test at the 95% level are shown in the top row for (a) 3 month precipitation (D_3); (b) 12 month precipitation (D_{12}); and (c) soil moisture (D_{sm}). For the grid cells where more than 2 of the models fail the test, the percentage of models which are drier (red) or wetter (blue) than the reference data are shown in the bottom row for (e) 3 month precipitation (D_3); (f) 12 month precipitation (D_{12}); and (g) soil moisture (D_{sm}). Grid cells where more than 80% of the members pass the test are not shown (white). (For interpretation of the references to color in this figure legend, the reader is referred to the web version of this article.)

gions, such as the south east, all of the HadRM3 ensemble members pass the K–S test. Fig. 3d shows whether the ensemble members which are significantly different from the reference data have distributions which are drier or wetter than the reference data at the point where the K–S test finds the greatest discrepancy between them. Grid cells where more than 70% of the ensemble members that fail are drier (wetter) than the reference data are shown in red (blue). Grid cells where less than 70% of the members that fail agree on the sign of the failure are shown in yellow. Grid cells where more than 80% of the members pass the test are not shown. In general, for D_3 the members that fail have distributions which are generally drier than the reference data. In the case of D_{12} (Fig. 3b), less than 75% of the ensemble members have distributions which are indistinguishable from the reference data. Again, as for D_3, the majority of members with different distributions are generally drier than the reference data at the point where the K–S test finds the greatest discrepancy between the distributions (Fig. 3e). In general, as the accumulation time increases the level of agreement between the modelled and reference distributions progressively decreases. The distribution of D_{sm} was compared with MPDM (Fig. 3c and f). Pass rates for soil moisture are much more spatially variable because the spatial patterns of the land surface characteristics are different for HadRM3 and for MPDM. Pass rates range from zero in north-west England and central Scotland to over 75% in south and west England. The HadRM3 ensemble members that fail are likely to be wetter than the MPDM drought indices. A similar comparison between RM40 and the HadRM3 ensemble (not shown) shows that RM40 generally falls within the spread of the model ensemble.

5.3. Historic drought

Fig. 4 shows examples of the relationship between return level or deficit and return period (Eq. (3)) for a grid cell in north-west

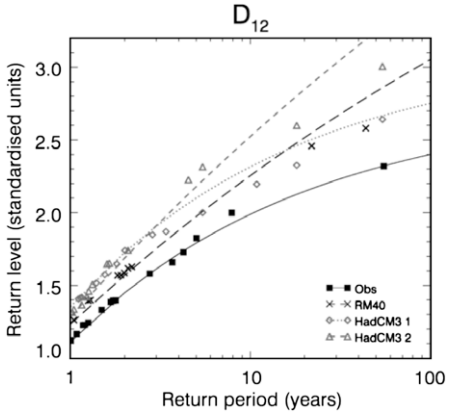

Fig. 4. The relationship between return level and return period of a grid cell in north-west Scotland for D_{12}. Observations, RM40 and 2 of the HadRM3 ensemble members are shown.

Scotland for D_{12}. Increasing positive values represent increasing deficit. The symbols represent the empirical ranking of dry months and the lines are the fitted stationary extreme value distributions (EVDs). Three members of the HadRM3 ensemble are shown along with the reference data and RM40. The return levels of the EVD for the reference data is 1.98 for 10 years; 2.19 for 25 years and 2.30 for 50 years. For this grid cell, at any given return period, the model ensemble generally has more severe droughts than the reference data. This is predominately due to the location parameter of the EVD (analogous to the mean of a normal distribution) being larger. The degree of curvature of the EVD is a result of both the scale and shape parameters and there are some notable differences in the value of these parameters for some of the ensemble members at this location. A similar analysis for a grid cell in southern England shows that the model ensemble generally has less severe droughts than in the reference data.

The spatial pattern of deficit is shown in Fig. 5 with maps of 25 year return levels of D_{12} and D_{sm} for both the reference data and RM40. These spatial fields have been smoothed using the median of nine nearest grid points; the centre and the surrounding eight. This reduces noise from differences in the parameters of the EVD resulting from fitting to relatively small samples. Return levels are in standardized units and, as for Fig. 4, the greater the value the more the deficit. UK average values for D_{12} are 2.67 for the reference data and 2.57 for RM40. There is a tendency for the precipitation drought index, D_{12}, to have greater deficit in the south and east than in the north and west. This gradient increases with increasing accumulation time. This is more prominent in RM40 than in the reference data largely because there are more extensive lower values in the west in RM40. D_{sm} (Fig. 5c and d) has greater deficits than D_{12} for this return period with UK-wide values of 3.13 for the reference data and 3.51 for RM40. The spatial patterns of the land surface characteristics also impact D_{sm}. Table 2 summarises these 25 year return levels over the UK expressed as a percentage of the 1961–1990 mean of the reference data. The UK-mean deficits (in standardized units) are relatively independent of accumulation time [not shown]. However, as might be expected, when return levels are expressed as a percentage of the reference data they depend on accumulation time. Spatial variations of the 25 year precipitation drought, illustrated here by the 5th and 95th percentile of the distribution of all UK grid points, are small compared with the differences between the accumulation times. RM40 has less severe precipitation drought (relative to the mean) than the reference data, suggesting that the climate model might have a tendency underestimate meteorological drought defined in this way. In contrast to the precipitation drought indices, D_{sm} has a wide range of values over the UK. This is comparable with the spread of all the precipitation drought indices. The RM40 soil moisture droughts are generally more severe than MPDM droughts and there is no distinct large scale spatial pattern again due to the dominant influence of land surface heterogeneity. In summary, RM40 and the reference data have return levels of similar orders of magnitude for any given return period with RM40 having more regular spatial variations than the reference data.

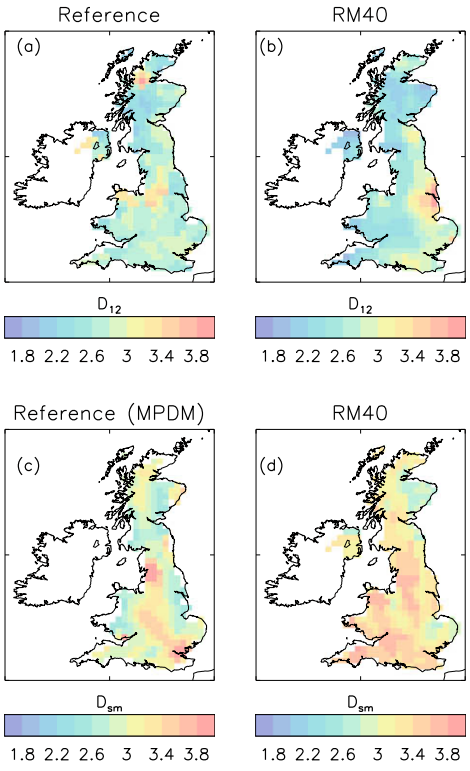

Fig. 5. The spatial variation of return level at a 25 year return period of the following drought indices: (a) 12 month reference precipitation; (b) 12 month RM40 precipitation; (c) reference soil moisture; and (d) RM40 soil moisture.

The ability of the model to reproduce the characteristics of dry months in the reference data was evaluated quantitatively on a grid cell and member basis over the reference period using the EVM method described in Section 4.2.1. Fig. 6 summarises the agreement between the model ensemble and the reference data and the model ensemble and RM40. Fig. 6a–d (top row) shows the percentage of ensemble members which are statistically indistinguishable from the reference data for D_{12} and D_{sm} together with comparisons between the ensemble and RM40. Most of the UK has pass rates of greater than 50%, though these range between 25% and 95%, depending on place. In general, pass rates are very similar for all precipitation drought indices and the RM40 soil moisture drought index. Regional differences are generally small, but pass rates are slightly better in the south when comparing the ensemble with the reference precipitation and RM40 soil moisture; and in central and northern England when comparing with RM40 precipitation. Pass rates are much lower when comparing the ensemble with MPDM with no ensemble members passing in the majority of central and southern Scotland. This improves over England to between 25% and 50%. An important reason for these differences is that the memory (serial correlation) of the MPDM drought indices is much larger than that in the model. For example, MPDM has serial correlations ranging from over 0.8 for 1-month lag times in the east to 0.5 in the north-west of Scotland compared with correlations of 0.5–0.3 for the standard version of the model. This difference in memory will impact the nature of extremely dry months so that the RCM soil moisture will respond more to short term precipitation variability than MPDM. Fig. 6e–h (bottom row) shows for the members that fail whether they have higher or lower return levels than either the reference data or RM40 at any given return period. This is calculated in a similar fashion to Fig. 3e–g. In the case of D_{12}, Fig. 6e shows that over Scotland the model is likely to be drier than the reference data whereas over England the model is likely to be wetter than the reference data. This is similar for RM40, but the drier region extends further south and west. In the case of D_{sm}, when significant difference is found, the ensemble members are drier than MPDM at any given return period. This may be because the model loses soil moisture too readily as reflected in the lower soil moisture serial correlation. As with RM40 precipitation, the ensemble members that fail are likely to be drier than the RM40 soil moisture in Scotland, whereas over England they are equally likely to be drier or wetter.

Table 2
Return levels (% of mean of reference data) for a 25 year return period for the reference data and RM40. The return levels were converted back to the original data by multiplying by the mean of the relevant 1961–1990 reference standard deviation and adding on the 1961–1990 reference mean and are expressed as a percentage of the relevant 1961–1990 reference mean. The mean value over the UK is shown along with the 5th–95th percentile of the distribution of values over the UK.

		3 months (%)	6 months (%)	12 months (%)	18 months (%)	Soil moisture (%)
Ref.	Mean	30.1	46.5	61.1	67.1	45.4
	5th percentile	21.6	33.4	54.5	60.3	17.5
	95th percentile	39.5	57.7	70.7	74.6	70.6
RM40	Mean	38.6	51.5	64.6	70.7	40.9
	5th percentile	31.1	44.0	58.5	64.5	22.1
	95th percentile	48.3	60.2	72.5	77.4	70.6

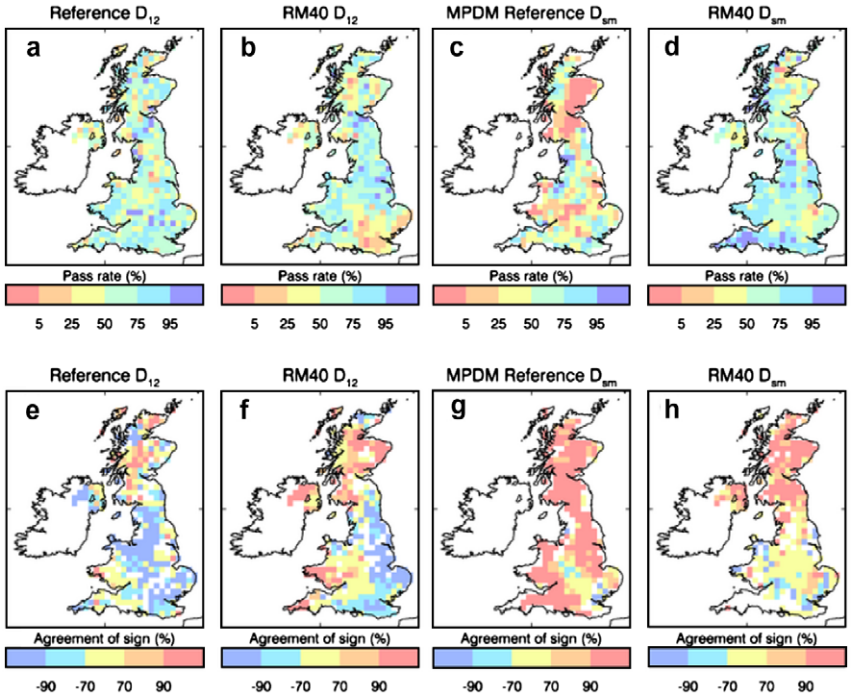

Fig. 6. The comparison of extreme value behaviour of the model ensemble and the reference data. The top row shows the percentage of models which have extreme value behaviour of dry months which is indistinguishable from (a) reference D_{12}; (b) RM40 D_{12}; (c) reference D_{sm}; and (d) RM40 D_{sm}. The bottom row shows, for the ensemble members that fail, the nature of the failure for (e) reference D_{12}; (f) RM40 D_{12}; (g) reference D_{sm}; and (h) RM40 D_{sm}. Places where more than 70% of the members show more (less) drought are shown in red (blue). Places where less than 70% of the members agree on either an increase or decrease are shown in yellow. Places were more than 80% of the members agree with the reference data are not shown (white). (For interpretation of the references to color in this figure legend, the reader is referred to the web version of this article.)

6. Future changes in drought

6.1. HadRM3 ensemble

In this section we use the HadRM3 ensemble to assess the potential range of changes in future drought for the UK over the 21st century, given that the ensemble has been able to capture many of the characteristics of the reference drought. This was done using the methodology described in Section 4.2.2. The preferred form of EVM [either (1) location or (2) location & scale dependent on global mean temperature] was found for each grid cell and drought index. Overall for D_3 and D_6 form (2) tends to be preferred with (1) preferred only occasionally. For the higher accumulation time precipitation drought indices (D_{12} and D_{18}) and for the soil moisture drought index (D_{sm}) form (1) is generally preferred in the south east; and form (2) in the north.

These preferred forms of EVMs are used to fit EVDs for individual ensemble members separately. The fitted EVDs for each ensemble members can then be used to calculate return levels as a function of global mean temperature for a given return period. An example of the evolving 25 year return level corresponding to 1950–2100 is given in Fig. 7 for a grid cell in southern England. Each line represents one ensemble member. Both the return levels

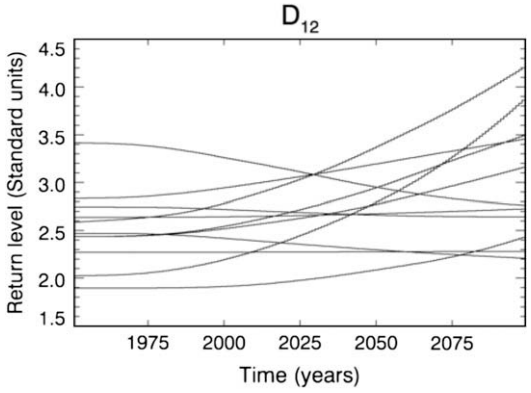

Fig. 7. Time series of the return level projected by the model ensemble for a 25 year return period between 1950 and 2100 for a grid cell in southern England. The preferred EVM is 'location and scale' and EVDs are found for each ensemble member.

and their changes are dependent on ensemble member. However, of interest here is the change in return level over time which can be combined with observed historic drought characteristics to give projections of future drought. For the majority of ensemble members there is an increase in return level (increasing deficit) over time. A few show little change or a slight decrease in return level. A similar analysis for a grid cell in north-west Scotland shows a decrease in return level over time for the majority of ensemble members.

Fig. 8 shows the spatial distribution of the projected change in return level at a 25 year return period for 2098 expressed as a percentage of the 2000 return level. For each drought index the range of changes projected by the 11 members are shown as all members are considered to be equally likely. For the vast majority of grid cells and drought indices, there can either be an increase or decrease in drought depending on ensemble member though the magnitude of the increases are generally much larger than the decreases. One exception is over south west England and Wales at shorter precipitation accumulation times, where all members project an increase in deficit. Another exception is over northern England and western Scotland at longer precipitation accumulation times, where the plausible decrease in deficit is a similar magnitude to the plausible increase. For nearly all grid points the ensemble range of changes in soil moisture drought span zero though for most of the UK the change is skewed to greater increases in drought. In all cases the ensemble mean has drought increasing for most regions.

Fig. 9 shows the distribution of the UK area averaged change in return level for each ensemble member. This is for a 25 year return period and changes between 2000 and 2098 expressed as a percentage of the 1961–1990 mean as in Table 2. The distributions show a definite increase in drought of up to an additional 20% of the 1961–1990 mean. This is slightly bigger for the shorter precipitation times than for the longer times and more variable for the soil moisture than for the precipitation.

6.2. An example: the 1976 drought

In order to put these changes into context the effect of the projections on a drought comparable to that of August 1976 was calculated. This section uses the reference data to quantify the deficit of the event of August 1976 and then determines the likelihood of a similar drought occurring under the future climate scenarios given by the HadRM3 ensemble.

Fig. 10 (first column) shows the spatial distribution of the return period (in years) of the reference drought in August 1976 calculated using the EVDs fitted to the reference data. The logarithm of the return periods was smoothed using the median of nine grid points as before. Any grid cell in black falls below the threshold used to fit the extreme value distribution (i.e. the 94th percentile). During August 1976, all drought indices show extremely dry conditions for the majority of the grid cells. However, the deficit at any one location is highly dependent on the drought index under consideration. In general, the south of England suffered a long term drought with return periods greater than 50 years in many places. On the shorter term, the drought was not particularly notable in this region. Central England, on the other hand, suffered both short and long term droughts. Longer term droughts are more likely to have significant impact on water resources with two dry winters significantly impacting both reservoir levels and groundwater levels. MPDM shows return periods of greater than 10 years for much the same region as D_{12}.

The effect of the changes projected in Section 6 on a drought such as that of August 1976 was calculated. This was done independently for each ensemble member and each grid cell. A 20th century return level for each ensemble member was derived for

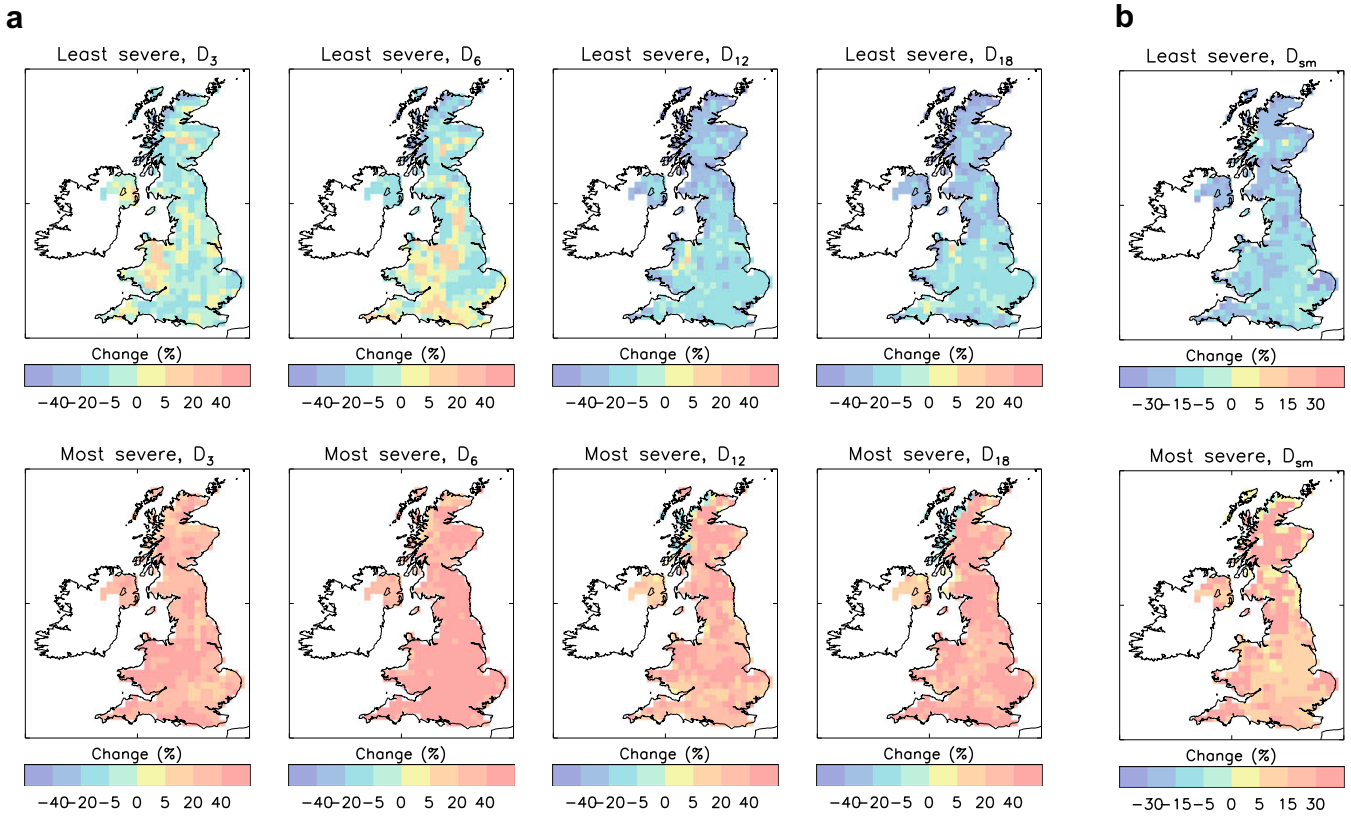

Fig. 8. The projected changes of each drought index in 2098 calculated by fitting the EVM to each ensemble member. The range of the changes in the return level at a 25 year return period is shown for the different precipitation and soil moisture drought indices. The change in return levels is expressed as a percentage of the return level in 2000.

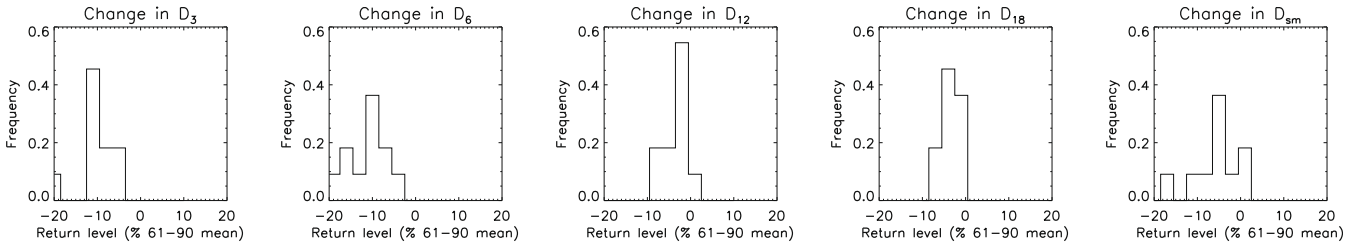

Fig. 9. The distribution of the area-mean change in the return level between 2000 and 2098 for the model ensemble. Return levels are expressed as a percentage of the 1961–1990 mean.

the return period of the 1976 drought calculated from the reference data and using the parameters of the stationary fit found for the period 1950–2000 for that ensemble member. These return levels were then used to calculate the evolution of the return periods through the century as a function of global mean temperature change using the preferred EVM and the fitted EVD for the relevant ensemble member. Fig. 10 (columns 2 and 3) shows, for the year 2098, the projected future return periods for events of the same magnitude as the 1976 event. As before, the regions in black were below the threshold for drought in the reference data and were not assessed for changes in this study. In general the 'least frequent' figure is very similar to the present day (column 2) which, for this example, provide an approximate upper limit on the return periods. The 'most frequent' figure shows the return period is projected to be less than once every 10 years. Results are similar for D_{sm}.

7. Discussion and conclusions

Drought occurs only rarely in the period of record. Therefore techniques which optimally use available information, such as extreme value analysis, are required in order to quantify accurately the likelihood of drought. This paper applies non-stationary extreme value theory to a range of drought indices to characterise present risk of observed drought and to make projections of how drought might change in the future for the UK. This is a novel approach which enables the risk of drought to be projected for any period in the current century using climate model data. A future extension of this method will be to adapt it to make probabilistic projections of drought, and it has been developed with this in mind.

A perturbed physics regional climate model ensemble was evaluated against observational-based reference data. The model ensemble generally underestimates the variability of precipitation in the historic climate but accurately models the extreme characteristics of the precipitation drought indices for over half of the ensemble members. When a climate model is evaluated for its suitability to make future projections under increased greenhouse gases it is commonly evaluated against a whole range of global metrics (Murphy et al., 2004). The global climate model ensemble on which these regional models are based has been shown to yield simulations of global climate of comparable quality to the standard published version of HadCM3 when compared with these global metrics (Collins et al., 2009). Each regional climate member is perturbed in a similar manner as its driving global model to maximise consistency between GCM and RCM. Mechanisms of change induced by increasing greenhouse gases are significantly influenced by remote feedbacks as well as local processes (Rowell, 2009). The driving global climate model ensemble was designed to capture uncertainties in key feedbacks which are themselves important mechanisms of change. Therefore, even though some of the regional climate model ensemble members have some difficulty reproducing the UK's climatology and variability, it is important to include them in this analysis to ensure the effects of these feedbacks are sampled.

Assessment of modelled soil moisture-based drought was hampered by the lack of direct soil moisture observations. There are notable differences between the regional climate model ensemble and a gridded version of a land surface model driven by high resolution meteorological analysis. One major reason for this is differences in soil moisture memory arising from the formulations of the two land surface schemes. A comparison of the regional climate model ensemble with a similar version of the regional climate model driven by an atmospheric reanalysis dataset shows good agreement. This provides evidence that the downscaling of the large scale atmospheric flow provided by the parent GCMs is not introducing significant bias.

In order to maximise data availability for the application of the extreme value theory, it was assumed that the standardized drought indices have the same extreme value characteristics independent of time of year and that they change in a similar fashion under future climate scenarios. However, for shorter duration droughts, changes may well be dependent on the time of year. This is particularly likely for soil moisture drought which depends on both evaporative demand and precipitation. Increases in evaporative demand may well have more effect on soil moisture in summer than winter. This impact of seasonality on projections of future drought has yet to be fully assessed.

Projections under increased greenhouse gases show an overall increase in drought occurrence. However, the spread is considerable ranging from little change or a slight decrease to a significant increase depending on drought index, ensemble member and, to a much smaller extent, location within the UK. This corresponds with the large uncertainties in projections found by both Blenkinsop and Fowler (2007) and Vidal and Wade (2009). In those papers, the authors projected an increase in short duration droughts over the UK. This is also projected by the majority of the perturbed physics ensemble members discussed here. Vidal and Wade (2009) also report a decrease in long term drought in Scotland. This is only found for a subset of ensemble members in this analysis, but, for those members, over a much larger proportion of the UK. This clearly highlights the high sensitivity of future UK drought prediction to climate modelling uncertainty and that the present state of climate prediction does not provide a well defined picture of future drought changes for adaptation planning.

Future projections are put into the context of the 1976 summer drought which had a significant impact on the UK. The likelihood of such a drought occurring in 2098 ranges from the same as the historic frequency to more frequently than once every 10 years, depending on ensemble member and drought metric. Such a future climate would require extensive changes to the water resources infrastructure of the UK and changes to water management policy.

There are three major sources of climate modelling uncertainty when estimating future climate change: as a result of (1) natural variability; (2) imperfect representation of the climate system within models; and (3) uncertainty in future emissions. Natural

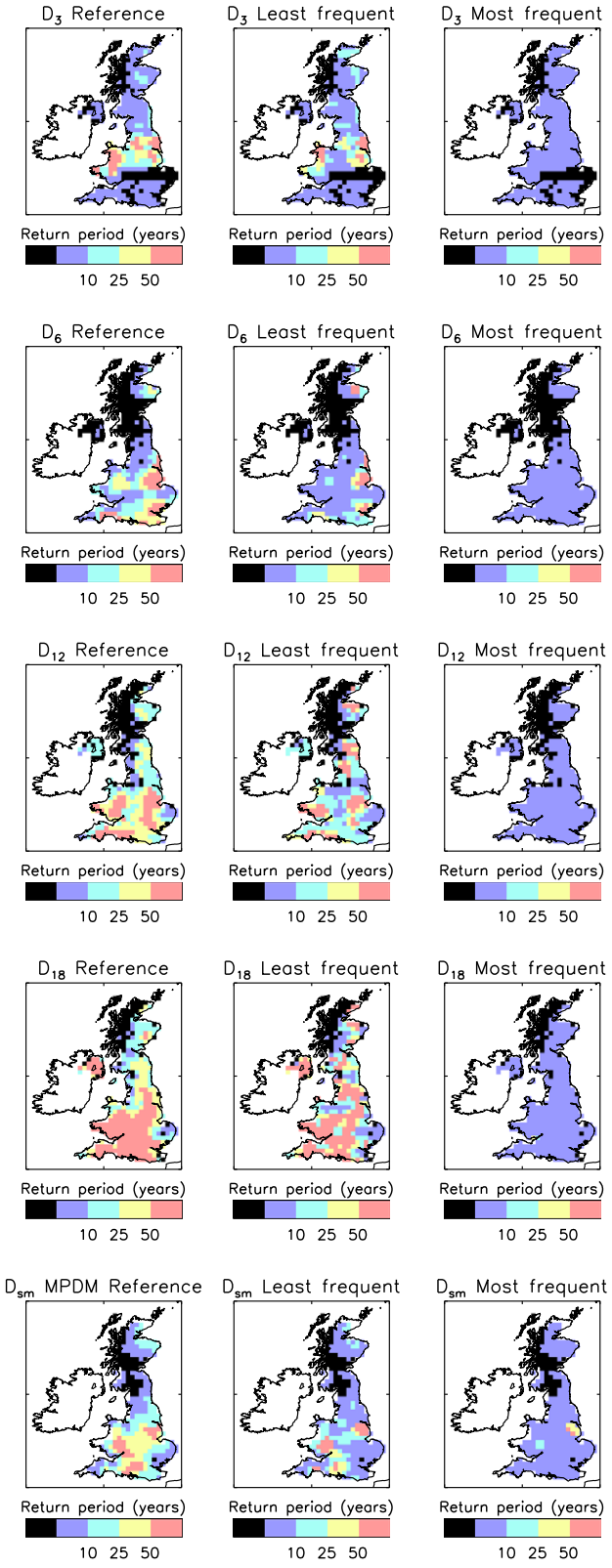

Fig. 10. The first column shows the return period (years) of the different observed drought indices for August 1976. Regions in black are not extreme in August 1976. The second and third columns show the least and most frequent estimates of future drought occurrence.

variability will be present as the climate evolves but can be characterised through extreme value theory. The perturbed physics ensemble was designed to ensure that all the key process uncertainties are sampled in a manner consistent with current scientific understanding. However, structural errors in the physical representation of the real climate system are not sampled (Murphy et al., 2004) requiring alternative methodologies for their inclusion such as using members of a multi-model ensemble. There is a need to develop methodologies to comprehensively describe these uncertainties and to account for variations in the credibility of alternative model versions to obtain a more robust estimate of the spread of future changes consistent with current knowledge and modelling capabilities in order to provide probabilistic projections on the changing risk of drought. Such a method has been developed for non extreme aspects of the climate developed for the UKCP climate projections (Murphy et al., 2009). Future work will focus on the application of this methodology on drought projections. This type of information will be required if the future risk of drought is to be effectively managed in national adaptation strategies to climate change.

Acknowledgements

This work was supported by the Joint DECC and Defra Integrated Climate Programme – DECC/Defra (GA01101). Additional funding was provided by WATCH (Contract Number 036946) an European Union (FP6) funded Integrated Project. We acknowledge the QUMP team at the Met Office Hadley Centre who created the multi-parameter ensemble and Dr. Robin Clark who was responsible for the regional climate model ensemble. The authors acknowledge the two anonymous reviewers who worked hard to improve the clarity of the paper.

References

Barnett, D.N., Brown, S.J., Murphy, J.M., Sexton, D.M.H., Webb, M.J., 2006. Quantifying uncertainty in changes in extreme event frequency in response to doubled CO_2 using a large ensemble of GCM simulations. Climate Dynamics 26. doi:10.1007/s00382-005-0097-1.

Blenkinsop, S., Fowler, H.J., 2007. Changes in drought frequency, severity and duration for the British Isles projected by the PRUDENCE regional climate models. Journal of Hydrology 342, 50–71.

Blyth, E.M., 2002. Modelling soil moisture for a grassland and a woodland site in south-east England. Hydrology and Earth System Sciences 6 (1), 39–47.

Brown, S.J., Caesar, J., Ferro, C.A.T., 2008. Global changes in extreme daily temperature since 1950. Journal of Geophysical Research-Atmospheres 113 (D5), D05115.

Christensen, J.H., Carter, T.R., Rummukainen, M., Amanatidis, G., 2007. Evaluating the performance and utility of climate models: the PRUDENCE project. Climatic Change 81. doi:10.1007/s10584-006-9211-6.

Clark, R.T., Brown, S.J., Murphy, J.M., 2006. Modelling northern hemisphere summer heat extreme changes and their uncertainties using a physics ensemble of climate sensitivity experiments. Journal of Climate 19, 4418–4435.

Coles, S.G., 2001. An Introduction to Statistical Modelling of Extreme Values. Springer. p. 225.

Collins, M., Booth, B.B.B., Bhaskaran, B., Harris, G.R., Murphy, J.M., Sexton, D.M.H., Webb, M., 2009. Climate model errors, feedbacks and forcings: a comparison of perturbed physics and multi-model ensembles. Climate Dynamics 27, 127–147.

Cox, P.M., Betts, R.A., Bunton, C.B., Essery, R.L.H., Rowntree, P.R., Smith, J., 1999. The impact of new land surface physics on the GCM simulation of climate and climate sensitivity. Climate Dynamics 15, 183–203.

Currie, I., 2008. The 1976 Drought. <http://www.bbc.co.uk/weather/features/understanding/1976_drought.shtml>.

Ekstrom, M., Jones, P.D., Fowler, H.J., Lenderink, G., Buishand, T.A., Conway, D., 2007. Regional climate model data used within the SWURVE project 1: projected changes in seasonal patterns and estimation of PET. Hydrology and Earth System Sciences 11 (3), 1069–1083.

Fowler, H.J., Blenkinsop, S., Tebaldi, C., 2007. Linking climate change modelling to impacts studies: recent advances in downscaling techniques for hydrological modelling. International Journal of Climatology 27 (12), 1547–1578.

Golding, B.W., 1998. Nimrod: a system for generating automated very short range forecasts. Meteorological Applications 5, 1–16.

Gordon, C., Cooper, C., Senior, C.A., Banks, H.T., Gregory, J.M., Johns, T.C., Mitchell, J.F.B., Wood, R.A., 2000. The simulation of SST, sea ice extents and ocean heat transports in a version of the Hadley Centre coupled model without flux adjustments. Climate Dynamics 16, 147–168.

Herbert, I., 2006. The Drought of 1976 Brought Standpipes and Shared Baths, The Independent. <http://www.independent.co.uk/environment/drought-of-1976-brought-standpipes-and-shared-baths-478513.html>.

Hingray, B., Mezghani, A., Buishand, T.A., 2007. Development of probability distributions for regional climate change from uncertain global mean warming and an uncertain scaling relationship. Hydrology and Earth System Sciences 11 (3), 1097–1114.
Jones, R.G., Noguer, M., Hassell, D.C., Hudson, D., Wilson, S.S., Jenkins, G.J., Mitchell, J.F.B., 2004. Generating High Resolution Climate Change Scenarios Using PRECIS. Met Office Hadley Centre, Exeter, UK.
Katz, R.W., Parlange, M.B., Naveau, P., 2002. Statistics of extremes in hydrology. Advances in Water Resources 25, 1287–1304.
Kharin, V.V., Zwiers, F.W., 2000. Changes in the extremes in an ensemble of transient climate simulations with a coupled atmosphere-ocean GCM. Journal of Climate 13, 3760–3788.
Kharin, V.V., Zwiers, F.W., Zhang, X.B., Hegerl, G.C., 2007. Changes in temperature and precipitation extremes in the IPCC ensemble of global coupled model simulations. Journal of Climate 20 (8), 1419–1444.
Koster, R.D., Guo, Z., Dirmeyer, P.A., Yang, R., Mitchell, K., Puma, M.J., 2009. On the nature of soil moisture in land surface models. Journal of Climate 22, 4322–4335. doi:10.1175/2009JCLI2832.1.
Marsh, T., Cole, G., Wilby, R., 2007. Major droughts in England and Wales, 1800–2006. Weather 62 (4), 87–93. doi:10.1002/wea.67.
Meehl, G.A., Stocker, T.F., et al., 2007. Global climate projections. I: climate change 2007: the physical science basis. Contribution of working group I to the fourth assessment report of the intergovernmental panel on climate change. In: Solomon, S., Qin, D., Manning, M., Chen, Z., Marquis, M., Averyt, K.B., Tignor, M., Miller, H.L. (Eds.). Cambridge University Press, United Kingdom and New York, NY, USA.
Murphy, J.M., Sexton, D., Jenkins, G., Boorman, P., Booth, B., Brown, K., Clark, R., Collins, M., Harris, G., Kendon, E., 2009. Climate Change Projections. ISBN: 978-1-906360-02-3.
Murphy, J.M., Sexton, D.M.H., Barnett, D.N., Jones, G.S., Webb, M.J., Collins, M., Stainforth, D.A., 2004. Quantification of modelling uncertainties in a large ensemble of climate change simulations. Nature 430, 768–772.
Nogaj, M., Yiou, P., Parey, S., Malek, F., Naveau, P., 2006. Amplitude and frequency of temperature extremes over the North Atlantic region. Geophysical Research Letters 33, L10801.
Perry, M.C., Hollis, D.M., 2005. The generation of monthly gridded datasets for a range of climatic variables over the UK. International Journal of Climatology 25, 1041–1054.
Pope, V.D., Gallani, M., Rowntree, P.R., Stratton, R.A., 2000. The impact of new physical parameterisations in the Hadley Centre climate model-HadAM3. Climate Dynamics 16, 123–146.
Rowell, D.P., 2009. Projected midlatitude continental summer drying: North America versus Europe. Journal of Climate 22, 2813–2833.
Smith, R.N.B., Blyth, E.M., Finch, J.W., Goodchild, S., Hall, R.L., Madry, S., 2006. Soil state and surface hydrology diagnosis based on MOSES in the Met Office Nimrod nowcasting system. Meteorological Applications 13 (2), 89–109.
Stainforth, D.A., Aina, T., Christensen, C., Collins, M., Faull, N., Frame, D.J., Kettleborough, J.A., Knight, S., Martin, A., Murphy, J.M., Piani, C., Sexton, D., Smith, L.A., Spicer, R.A., Thorpe, A.J., Allen, M.R., 2005. Uncertainty in predictions of the climate response to rising levels of greenhouse gases. Nature 433 (7024), 403–406.
Stott, P.A., 2003. Attribution of regional-scale temperature changes to anthropogenic and natural causes. Geophysical Research Letters 30 (14), 1728.
Sugahara, S., Porfírio da Rocha, R., Silveira, R., 2009. Non-stationary frequency analysis of extreme daily rainfall in Sao Paulo, Brazil. International Journal of Climatology 29 (9), 1339–1349.
Tallaksen, L.M., van Lanen, H.A.J., 2004. Hydrological Drought: Processes and Estimation Methods for Streamflow and Groundwater. Developments in Water Science, vol. 48. Elsevier, Amsterdam. p. 579.
Tebaldi, C., Mearns, L.O., Nychka, D., Smith, R.L., 2004. Regional probabilities of precipitation change: a Bayesian analysis of multimodel simulations. Geophysical Research Letters 31 (24), L24213.
Tomassini, L., Jacob, D., 2009. Spatial analysis of trends in extreme precipitation events in high-resolution climate model results and observations for Germany. Journal of Geophysical Research 114, D12113. doi:10.1029/2008JD010652.
Uppala, S.M. et al., 2005. The ERA-40 re-analysis. Quarterly Journal of the Royal Meteorological Society 131, 2961–3012.
Vidal, J.-P., Wade, S., 2009. A multimodel assessment of future climatological droughts in the United Kingdom. International Journal of Climatology. doi:10.1002/joc.1843.
Wainwright, M., 2006. The Great Drought, The Guardian. <http://www.guardian.co.uk/environment/2006/may/17/water.ethicalliving>.
Wang, A., Bohn, T.J., Mahanama, S.P., Koster, R.D., Lettenmaier, D.P., 2009. Multimodel ensemble reconstruction of drought over the continental United States. Journal of Climate 22, 2694–2712.
Webb, M.J. et al., 2006. On the contribution of local feedback mechanisms to the range of climate sensitivity in two GCM ensembles. Climate Dynamics 1, 2–10.1007/s00382-006-0111-2.
Wettstein, J.J., Mearns, L.O., 2002. The influence of the North Atlantic–Arctic Oscillation on mean, variance, and extremes of temperature in the northeastern United States and Canada. Journal of Climate 15, 3586–3600.
Zhang, X.B., Zwiers, F.W., Li, G.L., 2004. Monte Carlo experiments on the detection of trends in extreme values. Journal of Climate 17, 1945–1952.